Marine Geology, 116 (1994) 113–132
Elsevier Science B.V., Amsterdam

Geology and geochemistry of a 800 m section through young upper oceanic crust in the North Fiji Basin (Southwest Pacific)

Yves Lagabrielle[a], Jean-Marie Auzende[b,1], Jean-Philippe Eissen[c], Marie-Christine Janin[d] and Joseph Cotten[a]

[a]*URA CNRS 1278 and GDR "GEDO", Faculté des Sciences, Université de Bretagne Occidentale, 6, Avenue Le Gorgeu, 29287 Brest Cédex, France*
[b]*IFREMER, Centre de Brest and GDR "GEDO", B.P. 70, 29280 Plouzané, France*
[c]*ORSTOM, Centre de Brest and GDR "GEDO", B.P. 70, 29280 Plouzané, France*
[d]*CNRS and Université P. and M. Curie, Laboratoire de Micropaléontologie, 4, Place Jussieu, T15, E4, 75252 Paris Cédex 05, France*

(Received October 2, 1992; revision accepted June 14, 1993)

ABSTRACT

Lagabrielle, Y., Auzende, J.-M., Eissen, J.-P., Janin, M.-C. and Cotten, J., 1994. Geology and geochemistry of a 800 m section through young upper oceanic crust in the North Fiji Basin (Southwest Pacific). In: J.-M. Auzende and T. Urabe (Editors), North Fiji Basin: STARMER French–Japanese Program. *Mar. Geol.*, 116: 113–132.

We report the results of geological and structural observations made during one dive of the French submersible *Nautile* during the STARMER Cruise in 1989 in the vicinity of the 16°40'S triple junction in the North Fiji Basin. This dive provided a spectacular, 800 m continuous section of oceanic crust exposed along the northern wall of a 3000 m deep basin at the eastern branch of the triple junction. A number of volcanic facies have been encountered including massive and pillowed lavas, sheeted dikes and spectacular columnar-jointed massive lavas. Pillowed lavas have been observed only at the base and at the top of the section. The ratio between massive and pillowed basalts is high suggesting that the crust in this area grew mostly during a stage of high eruptive rate. Dikes have been observed in the middle part of the section. They probably do not represent the top of a classical "dike complex" but an isolated set of sheeted dikes, possibly the feeders of overlying flows. The abundance of vertical tectonic breccias observed during the first part of the dive confirms that the basal part of the wall can be regarded as a major tectonic boundary along which occurred significant vertical and strike-slip motions. Micropaleontological data from sedimentary rocks collected during the dive bring new constraints to the evolution of the triple junction. The oceanic crust in the surveyed area is at least as old as 1.9–1.3 Ma, based on the age of sedimentary rocks collected in talus at the base of the wall and observed at the summit of the section. The collected basalts include (1) N-type MORBs, (2) E-type MORBs and (3) BABBs. This emphasizes the heterogeneous nature of the mantle beneath the central NFB. Some portions of the depleted mantle underlying the central NFB triple junction area have recorded contamination from melts or fluids from an ancient subduction zone (probably the New Hebrides during the opening of the NFB), whereas adjacent mantle areas show the influence from an alkali-enriched source. Such alkali-enriched characters are reported from recent basalts of the northern NFB (South-Pandora ridge–Rotuma island).

Introduction

During the last 10 years, in situ geological studies of cross-sections through oceanic crust and mantle have become more frequent. However, extended continuous sections of very young oceanic crust have been rarely explored in major ocean as well as in marginal basins because important reliefs allowing continuous exposure within the axial domains of the oceanic ridges are uncommon. The Hess Deep in the eastern Pacific (Francheteau et al., 1992), the Blanco Trough in the northern Pacific (Juteau at al., 1991) and

[1]Present address: Laboratoire de Géologie et Géophysique, UR1F, ORSTOM, B.P. A5, Nouméa, New Caledonia

0025-3227/94/$07.00
SSDI 0025-3227(93)E0099-R

various ridge–transform fault intersection domains in the Atlantic are the only areas located very close to active spreading axis of major oceans that have allowed extended sections of very young oceanic crust to be explored (OTTER, 1985; Karson and Dick, 1983; Auzende et al., 1990a; Mével et al., 1991; Mamaloukas-Frangoulis et al., 1991; Lagabrielle et al., 1992). In this paper, we report the results of submersible investigation of a spectacular submarine cliff located very close to a present-day spreading axis in the North Fiji Basin. This demonstrates that back-arc basins also provide the opportunity to carry out in situ studies of very young oceanic crust, thus leading to a better understanding of the internal structure and compositional variations of the oceanic lithosphere in such environments.

Over the last 5 years, bathymetric surveys using multibeam echosounders and SeaMARC II side scan sonar (*Seapso* 3, *Kaiyo* 87, 88 and 89, *Moana Wave* 87 and *Yokosuka* 90 cruises) as well as submersible investigations (STARMER I and II, *Yokosuka* 91) have revealed the complex pattern of the central spreading axis of the North Fiji Basin (NFB) (Kroenke et al., 1987; Auzende et al., 1988a,b, 1989, 1990b, 1991a,b; Ruellan et al., 1989; Lafoy, 1989; Lafoy et al., 1990). A number of cruises have been conducted in the area around 16°S, 173°E where a triple junction has been mapped in detail. Here, the western tip of the E–W trending North Fiji Fracture Zone (NFFZ) connects the northern and the southern branches of the central spreading axis of the NFB, trending N160° and N15°, respectively (Fig. 1). The eastern branch of the triple junction which corresponds to the western terminaison of the NFFZ is a triangular-shaped graben with a relatively flat floor. In its western part, close to the triple junction, this triangular basin is bounded to the north and to the south by two steep walls up to 1000 m high (Figs. 2–4).

During the STARMER I cruise of the French submersible *Nautile* in 1989, nine dives were conducted in the vicinity of the 16°40'S triple junction. Dives 1–6 were carried out along the N15° trending axial graben of the southern branch of the triple junction where the hydrothermal active site "White Lady" has been surveyed in detail (Auzende et al., 1989, 1991; Grimaud and Ishibashi, 1991; Bendel et al., 1991). Dives 7–9 were conducted in the graben located along the eastern branch of the triple junction (Fig. 4).

We report the results of geological and structural observations made during dive no. 7 along the northern wall of this graben, providing a spectacular section through upper oceanic crust (Figs. 5

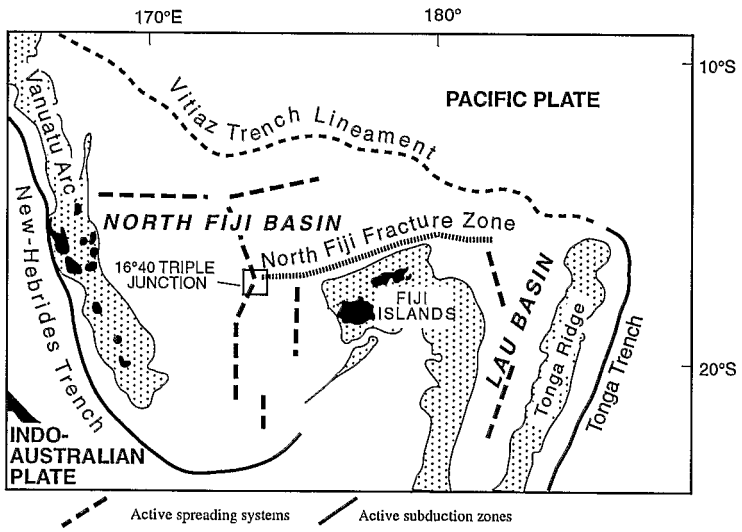

Fig. 1. Simplified map of the Lau–Fiji Basin region and location of the central triple junction in the North Fiji Basin.

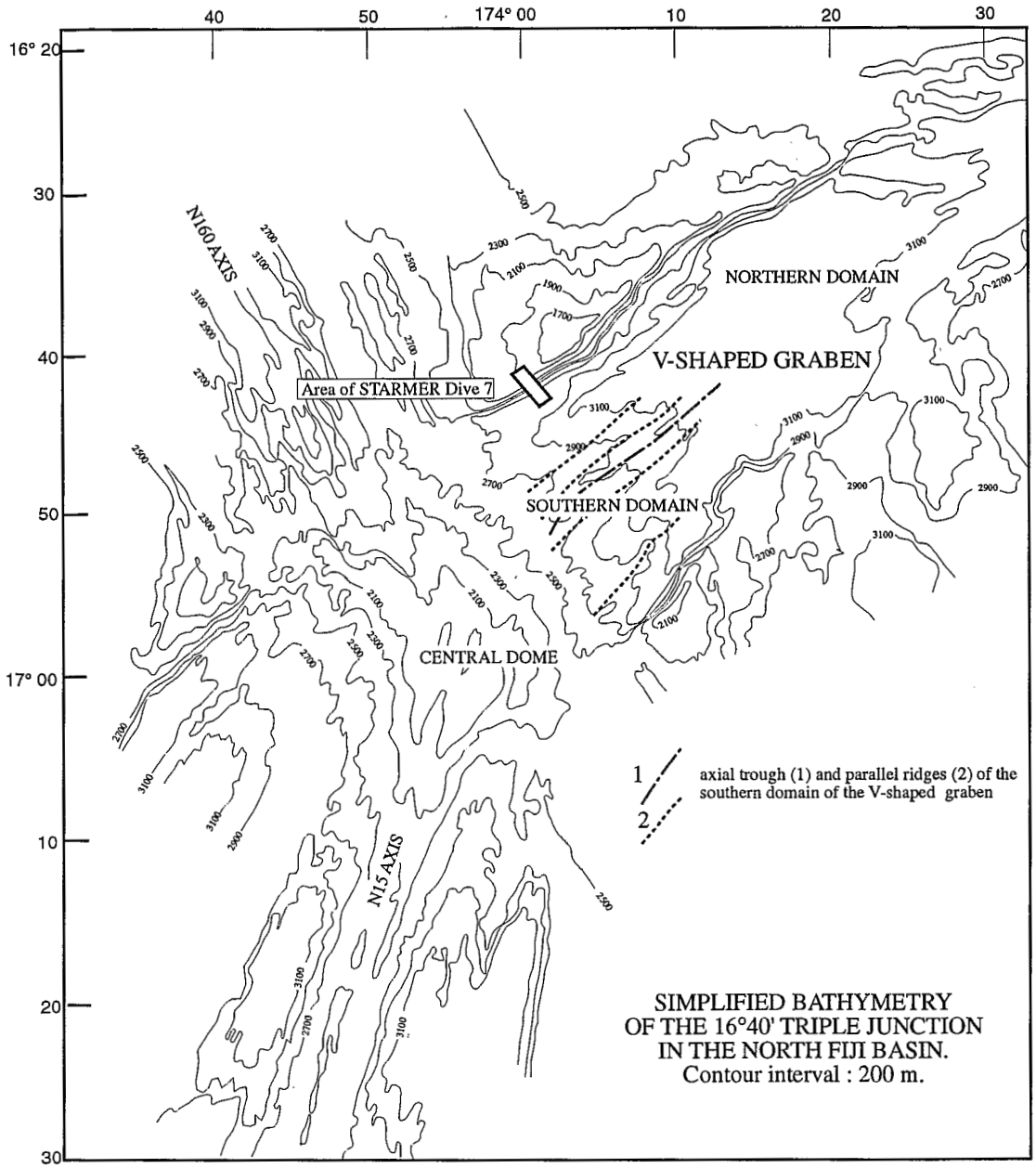

Fig. 2. Bathymetry of the central (16°40'S) triple junction in the North Fiji Basin.

and 6). Micropaleontological data from sedimentary rocks collected during the dive are presented together with petrologic and geochemical analyses of lavas and dikes. These results bring new constraints to the evolution of the triple junction.

1. The 16°40'S triple junction in the North Fiji Basin

General presentation

The 16°40'S triple junction in the central region of the North Fiji Basin is the area where the N15°

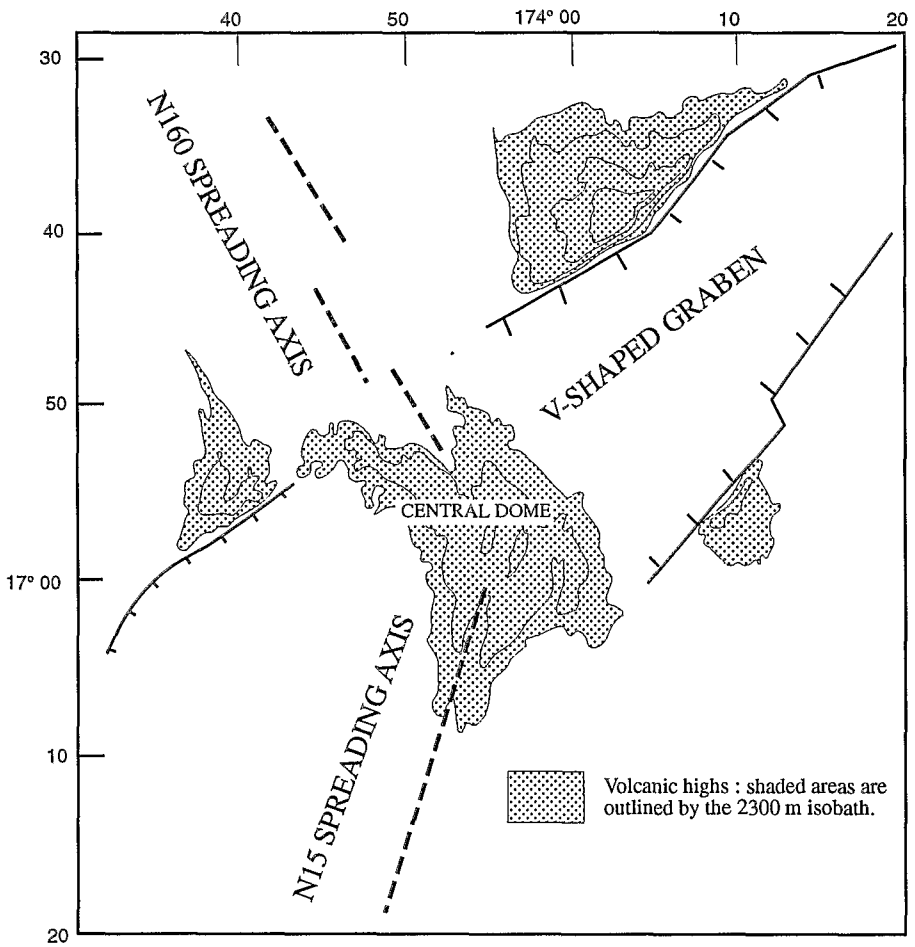

Fig. 3. Simplified sketch of the triple junction area and location of the volcanic highs.

and N160° active spreading axis connect with the western end of the North Fiji Fracture Zone (NFFZ) (Fig. 1). The central region of the triple junction corresponds to a shallow volcanic dome, culminating at less than 1900 m below sea level, and lying at about 500–600 m above the surrounding seafloor (Fig. 2). The dome is cut by a 2 km wide central graben. This graben represents the northern prolongation of the axial graben of the N15° spreading axis. The central dome deepens progressively toward the northern arm of the triple junction which corresponds to the N160° spreading axis. This spreading axis consists of a series of parallel ridges and of en echelon central grabens, locally more than 4000 m deep (Auzende et al., 1991b). To the east, the central dome deepens toward a V-shaped graben forming the eastern arm of the triple junction at the tip of the NFFZ.

One of the main characteristics of the 16°40'S triple junction region is the presence of high reliefs of volcanic origin. These topographic anomalies are well defined by the 2300 m isobath (Fig. 3). They include the recent volcanic dome occupying the central region and an elongated ridge located northwest of the central dome. This ridge also connects to a N40° trending, curvated ridge lying to the west of the triple junction. To the east of the triple junction, high reliefs are found on both edges of the V-shaped graben. They consist of two large, hemi-circular topographic anomalies which appear to have been cut by the fault system bounding the V-shaped graben. The half-dome

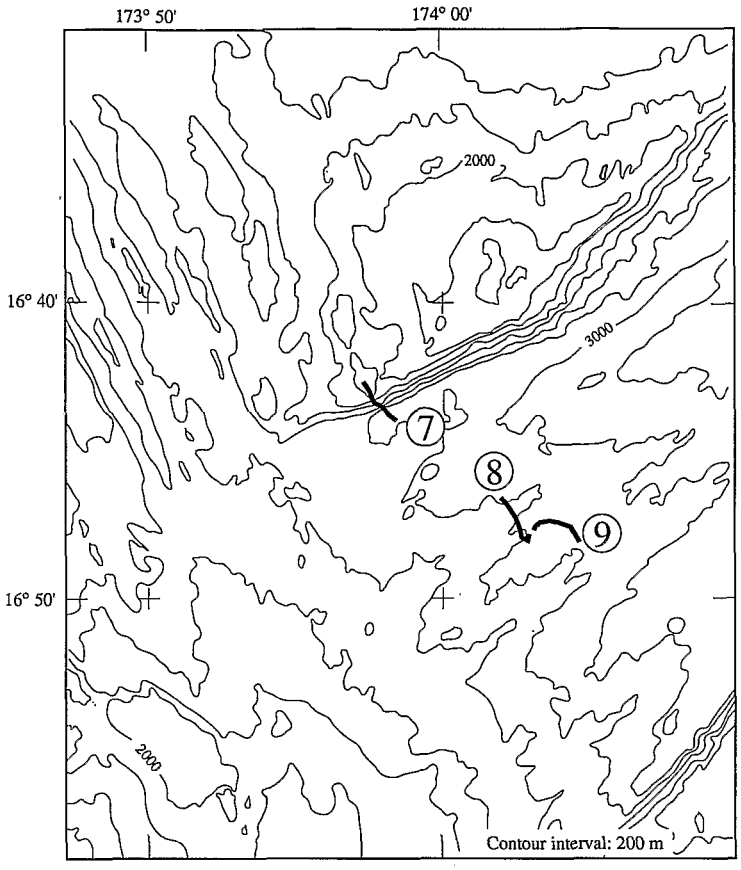

Fig. 4. Detailed bathymetry of the eastern arm of the triple junction area with the locations of STARMER I dives *7*, *8* and *9*.

located along the northern wall of the graben culminates at 1600 m below sea level. Dive no. 7 was conducted along the northern wall of the graben, at the foot of this half-dome, thus providing a natural cross-section through this constructional feature (Fig. 4).

The V-shaped graben at the eastern arm of the 16°40'S triple junction

The deep graben observed at the western tip of the NFFZ has been surveyed in detail during the *Kaiyo* 87 cruise (K1 box; Auzende et al., 1988a,b; Lafoy, 1989). It shows a general triangular outline with a maximum width of 40 km and a 70 km long axis (Fig. 2). It is delineated by a set of N60° and N40° striking structures, and can be divided into two different domains.

The southern domain exhibits a triangular contour (Fig. 2). It is connected to the triple junction along its western boundary and is bounded to the north and to the south by two 1000 m high, steep walls, trending N60° and N40°, respectively. In this domain, the floor of the graben deepens progressively from 2200 m near the triple junction to 3400 m to the east. It shows a succession of four parallel, N60° trending, moderately elevated ridges. A 20 km long axial trough is present between the two central ridges. The outline of the ridges and axial trough clearly defines a V-shaped topographic feature, with axial symmetry, resembling structural patterns described at the tip of propagating rifts (Fig. 2). Conical seamounts, probably recent volcanoes, are abundant on the floor of the graben, suggesting an important volcanic activity. During STARMER dives no. 8 and 9 conducted in the axial trough and across the northern flank of the axial zone of this domain

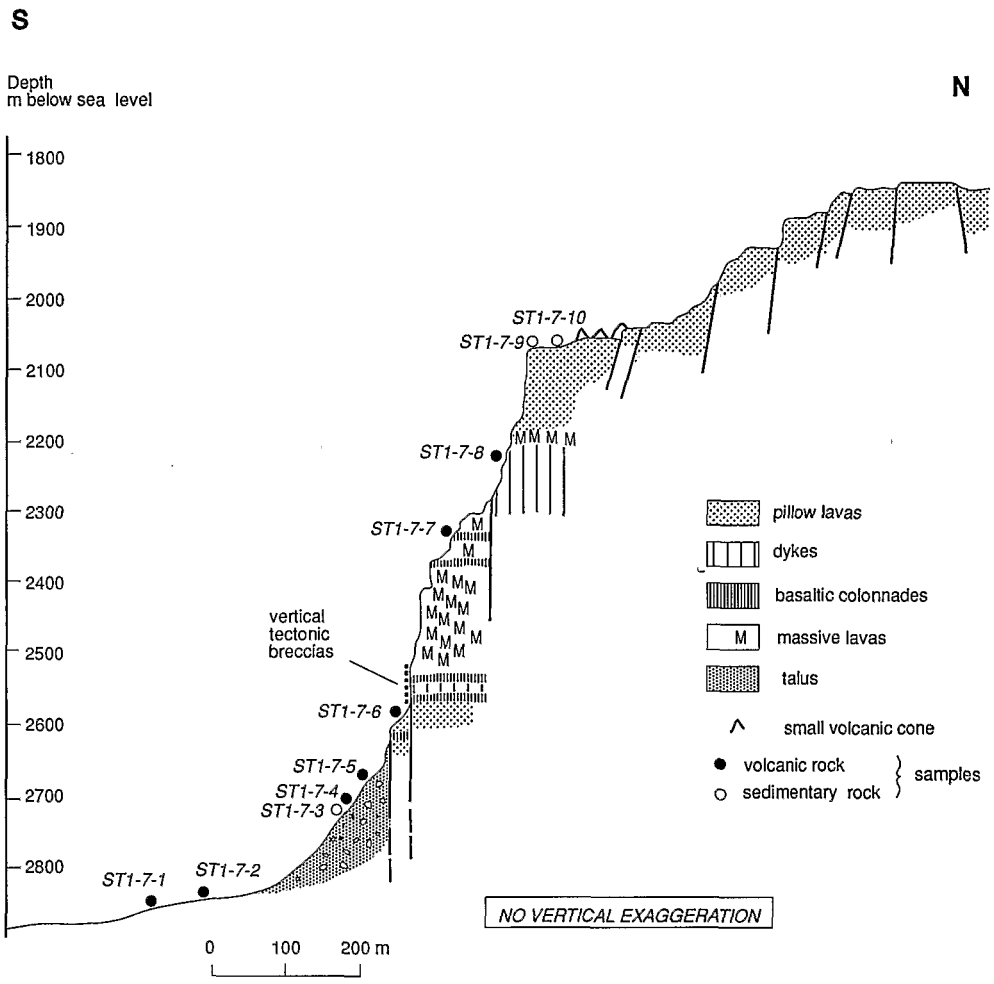

Fig. 5. Geological cross-section observed during dive 7 (without vertical exaggeration). The location of the samples collected is shown by dots.

(Fig. 4), freshly emplaced lava lakes and lava tubes were observed, as well as numerous marks of recent tectonic activity. Such observations are in agreement with the high reflectivity of the SeaMARC II image of this area (Kroenke et al., 1987), and confirm that this graben has been tectonically and magmatically active in very recent times. It has been suggested that the propagation of a limited rift may have occurred very recently within the floor of the graben (Lafoy et al., 1990). According to spreading rates calculated along the northern and southern spreading axes (Auzende et al., 1990), the propagation occurred probably within the last 400,000 years.

The northern domain of the graben corresponds to a deep, flat-floored, polygonal area with a more than 3300 m average depth, lying along the north-eastern side of the former domain. It shows a well-defined northern boundary corresponding to two successive steep walls trending N20° and N40° in connection with the northern boundary of the former domain. The southern limit of the second domain is more diffuse and can be defined as a 10 km wide zone of gently northwest dipping slopes comprised between isobaths 2700 and 3300 m. Due to the lack of in situ observations, little can be said regarding the nature and origin of this second domain. Seismic reflection profiles show that this area is filled with sediments (maximum thickness: 200 ms) (Lafoy, 1989) suggesting that the crust

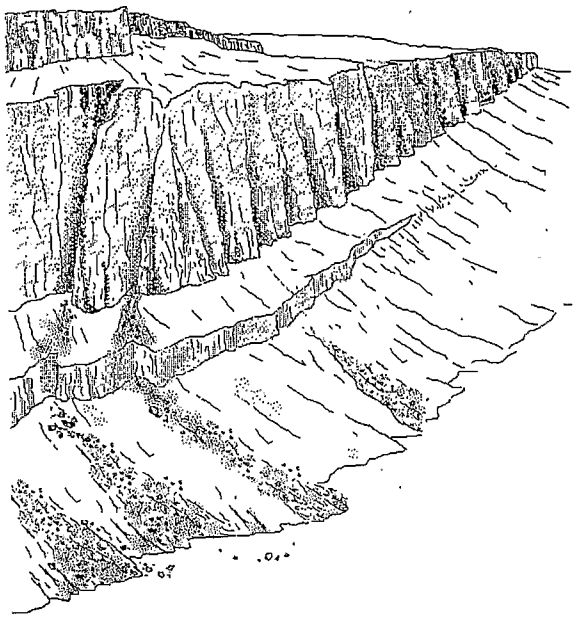

Fig. 6. Artistic view of the northern cliff along which dive 7 was conducted.

has not been created recently. We suggest that this domain originated as a pull-apart basin related to a major left-lateral motion of the NFFZ, before rift propagation.

2. Morphological and geological observations during STARMER I dive no. 7

The dive started at 2880 m in a flat area covered with white pelagic muds, located at 900 m south of the base of the northern wall of the graben. Average heading during the dive was N340° and total time on seafloor was 5h10.

The slope increases gently from the start point to the base of the wall (Fig. 5). As approaching the wall, isolated blocks of lavas (samples ST1-7-1 and -2) and of layered consolidated sedimentary rocks become abundant. The size of isolated blocks also increases upslope. Groups of few meter-sized blocks scattered on the pelagic muds have been observed at 2824 m.

The base of the wall (2816 m) consists of an unstable, steep talus (slope: 45°) composed of decimeter-sized pillow fragments (samples ST1-7-4 and -5) (Plate Ia). Some 50–100 m wide, elongated zones paralleling the slope direction are devoid of any basaltic debris. Numerous angular blocks of layered consolidated sedimentary rocks with size ranging from one to few meters have been observed on the talus (sample ST1-7-3) (Plate Ib). Some of their surfaces show cross-cut striations probably caused during the gentle, downslope rafting of the blocks over the basaltic debris. The summit of this talus marking the base of the wall was reached at 2620 m, the total thickness of the detrital formation is thus 200 m.

On the upper slope we observed a 300 m high cliff, exposing basaltic rocks. The general trend of the cliff is N40° but it shows a complex detailed topographic pattern with numerous secondary cliffs showing various orientations (N20° to N60° and N110°–120°). These secondary cliffs are joined by sharp spurs or deep channels with directions ranging from N0°–20° to N140°. These features are associated with very steep unstable slopes covered with angular basaltic debris and pelagic sediments (Fig. 5).

Densely fracture massive flows with local aspect of cataclastic breccias are exposed at the base of the wall along a vertical N20° trending cliff at 2620 m. Sections of pillows were observed upslope from 2600 to 2587 m (sample ST1-7-6). Massive, columnar-jointed flows are exposed at 2587 m; they underlie pillow lavas which are exposed at 2547 m along a N120° oriented vertical cliff. A clear schistosity can be observed in large pillows exposed at the foot of the cliff. It consists of a succession of parallel planes dipping 60° to the south with a N60° direction. A vertical major fault oriented N40°–60° can be observed at 2539 m. On the northern edge of the fault plane, the rocks, probably massive basalts, also show pervasive tectonic cleavage. Rocks outcropping along the southern side of the fault are tectonic breccias with angular blocks ranging in size from a few centimeters to one meter, also showing weak schistosity. The geometrical relationships between the fault plane (gliding plane) and the cleavage planes (schistosity) are compatible with a normal sense of shear along the fault. Vertical tectonic breccias are exposed almost continuously up to 2513 m. At 2500 m a vertical, N60° trending fault surface exposes massive basalts showing horizontal striation related to strike-slip displacement.

PLATE I

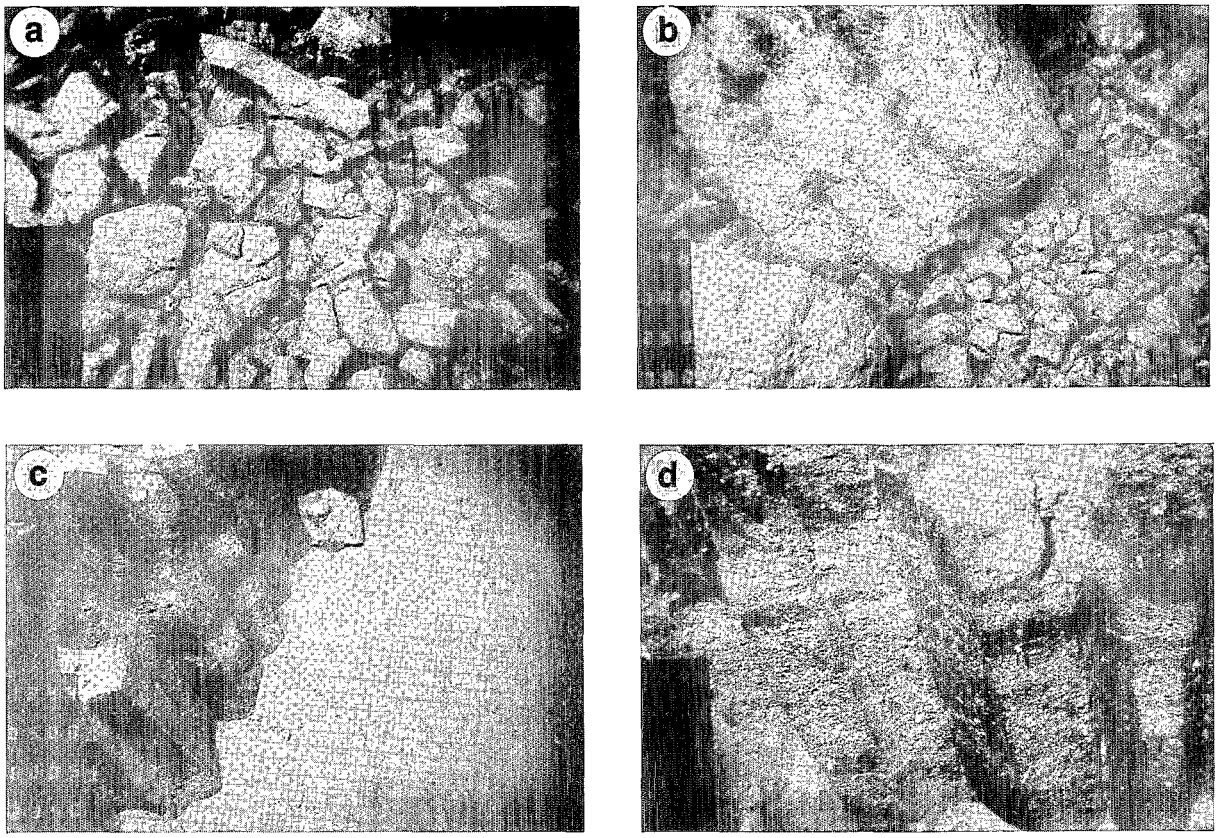

Bottom photographs taken during dive no. 7 of the *Nautile*, STARMER I cruise in the area of the 16°40'S triple junction. (a) Unconsolidated talus composed of angular blocks of basalts and dolerites observed at the bottom of the northern wall surveyed during dive no. 7. (b) Isolated block of layered, sedimentary rock, lying on a talus similar to that shown on photograph (a), at the foot of the wall. Such a block probably comes from the sedimentary carapace of the basaltic plateau surveyed during the last part of the dive. (c) and (d) A typical aspect of the columnar-jointed basaltic sheet flows observed at 2341 m water depth along the wall.

Highly fractured massive basalts are exposed from 2500 to 2330 m (sample ST1-7-7) along a succession of vertical cliffs separated by ensedimented slopes and sharp spurs. Numerous vertical faults can be observed, corresponding to deep fractures trending from N10° to N60°. Locally, 1–2 m thick, vertical fault breccias similar to the breccias exposed from 2539 to 2513 m can be observed.

At 2339 m depth, we observed spectacular outcrops of columnar-jointed basalts (Plate Ic and d). The prisms are 2–3 m high and have 20–30 cm wide well defined surfaces. Well-exposed colonnades also occur upslope above a sedimented talus. They are overlain by massive, fractured basalts, which can be observed at 2279 m along a vertical cliff. A gentle, sedimented slope was observed between 2300 and 2260 m of water.

A complex of sheeted dikes is present along a 20 m long, almost vertical outcrop at 2253 m depth (Plate IIa). Thickness of dikes is around 1 m and their margins are trending N340° with an average dip of 60° toward the west (sample ST1-7-8). From 2150 m to 2039 m basaltic flows overlain by a 100 m thick sequence of pillows are exposed continuously along an almost vertical cliff. Isolated dikes and possible sills cross-cutting pillows are observed at 2138 m. The size of pillows decreases significantly toward the top of the cliff (Plate IIb).

A 300 m wide flat terrace representing the upper

PLATE II

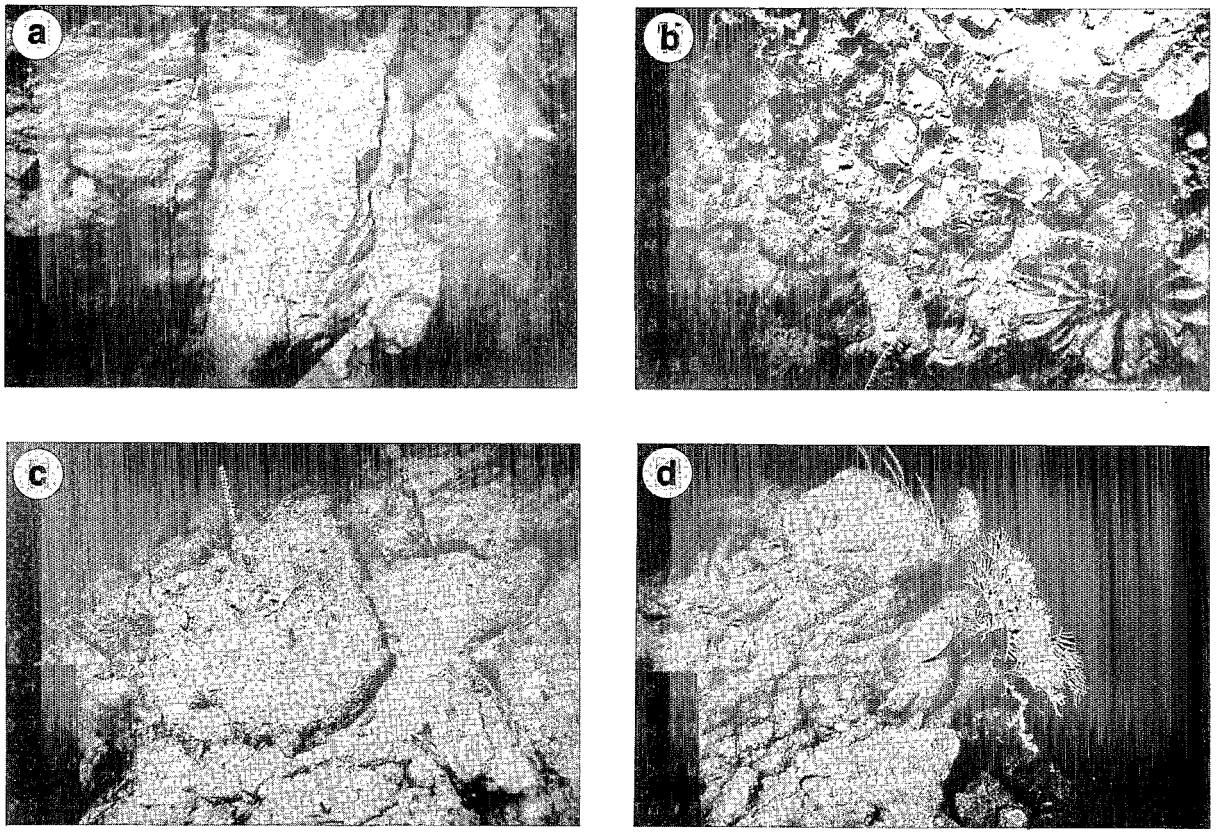

Bottom photographs taken during dive no. 7 of the *Nautile*, STARMER I cruise in the area of the 16°40'S triple junction. (a) Aspect of the sheeted dikes observed at 2253 m water depth in the upper part of the section. (b) Typical sections of pillowed lavas observed near the summit of the wall at 2138 m water depth. (c) An aspect of the flat terrace representing the upper surface of the upper most pillow formation (2036 mbsf). The surface is capped with consolidated sedimentary rocks forming a 1–2 m thick, brittle carapace broken by place into polygonal flakes. (d) A few meters high, conical-shaped volcanic edifice with radial sets of down-flowing tubes observed on the terrace floor. The lavas have been emplaced locally over the sedimentary carapace (2032 mbsf).

surface of the pillow formation observed below is present at 2038 m. The terrace is capped with consolidated sedimentary rocks forming a 1–2 m thick, brittle carapace (Plate IIc) (sample ST1-7-9). This sedimentary cover is broken by place into polygonal meter-sized flakes (sample ST1-7-10), most probably in relation with fault affecting the underlying basement. Local compressional deformation is evidenced by bending, fracturing and thrusting of the sedimentary crust.

Conical-shaped volcanic edifice, a few meters high, showing radial sets of down-flowing tubes are spotted on the terrace floor (Plate IId). They indicate that lavas have been emplaced locally over the sedimentary carapace.

Three major vertical fault scarps, 40–50 m high, cutting through small-sized pillows and trending successively N60°, N60°–70°, and N110° were observed during the last part of the dive. At 1956 m a soft fault surface exposes well-marked striation. The average striation pitch is 45° toward the southwest. This confirms that both normal and strike-slip displacements occurred along the edge of the graben.

3. Micropaleontological study: Age of the sediments

Three samples of sedimentary rocks have been collected during the dive. Sample ST1-7-3 is a moderately lithified, yellowish calcareous mudstone containing calcareous nannofossils and planktonic foraminifera. A thin manganese crust is preserved locally. This sample is part of a block from the scree deposits observed at the foot of the basaltic cliff at the beginning of the dive. Samples ST1-7-9 and ST1-7-10 are calcareous mudstones collected in situ from the sedimentary carapace outcropping on the terrace at 2038 m depth. Sample ST1-7-9 is heterogeneous (Fig. 7). It consists of a brownish calcareous mudstone (ST1-7-9a) with poorly preserved microfossils, showing numerous burrows infilled with light calcareous ooze containing well preserved nannofossils (ST1-7-9b). Its surface is capped by a manganese crust up to 8 mm thick, which clearly developed after burrowing. Poorly consolidated calcareous mud from a molluscan shell attached on the manganese crust contains calcareous nannofossils, planktonic foraminifera, diatoms, radiolarians and silicoflagellates (ST1-7-9c). Sample ST1-7-10 is homogeneous and shows a similar aspect to that of sample ST1-7-3. It contains well preserved and rather abundant calcareous nannofossils and planktonic foraminifera.

Age determinations are based on micropaleontological analyses of the calcareous nannofossils. The samples yield well defined assemblages similar to that previously described in the Fiji basin (Edwards, 1973). Figure 8 shows the stratigraphic positions of the three samples with respect to the calcareous nannofossil zonations by Martini and Müller (1986) and Okada and Bukry (1980) together with the estimated ages according to Hills and Thierstein (1989). Taxonomic references are taken from Perch-Nielsen (1985).

The three studied samples are characterized by the absence of *Discoaster* which is typically abundant in Pliocene sediments from tropical oceanic environments. This indicates that all the assemblages belong to the Pleistocene. Sample ST1-7-3 contains both *C. leptoporus* s.s. and *C. macintyrei*

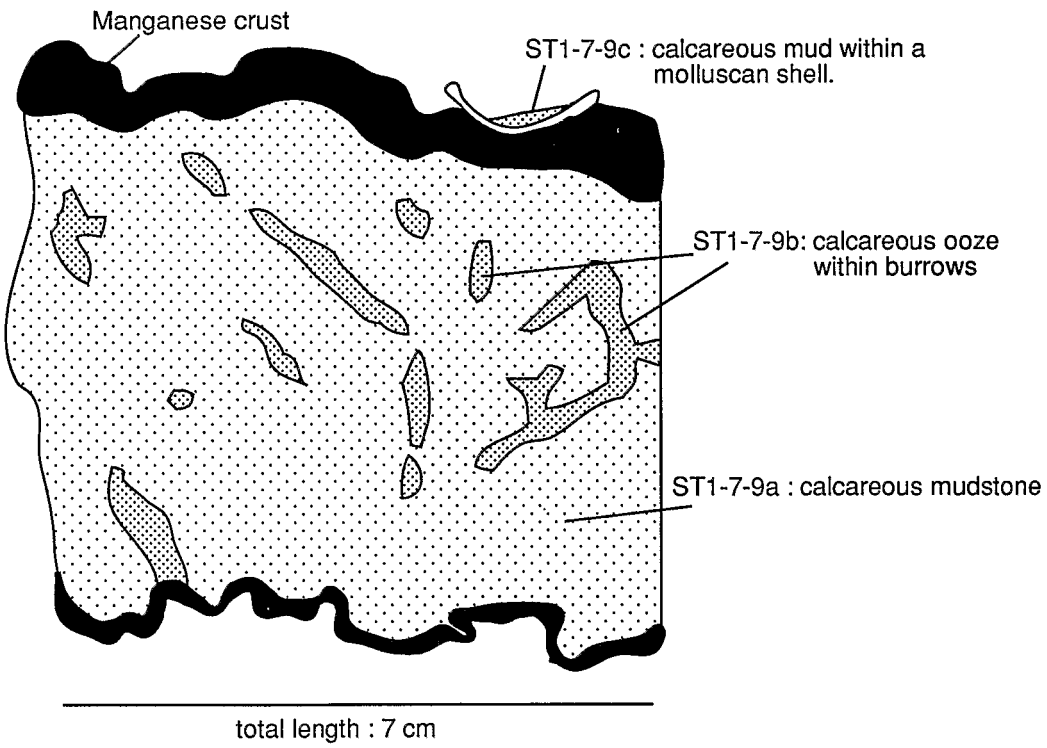

Fig. 7. Simplified representation of a section of sample ST1-7-9.

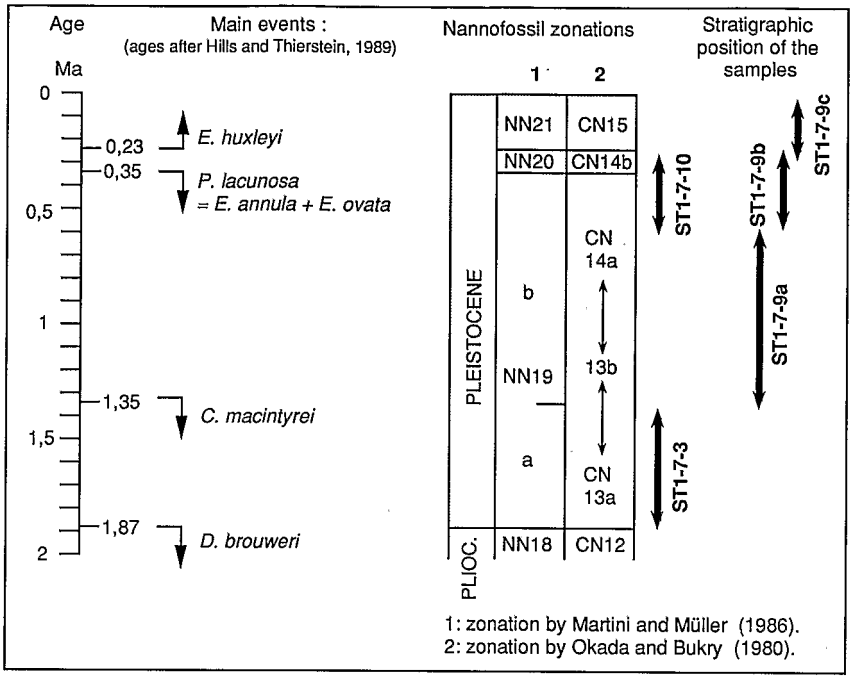

Fig. 8. Age of the calcareous nannofossils assemblages.

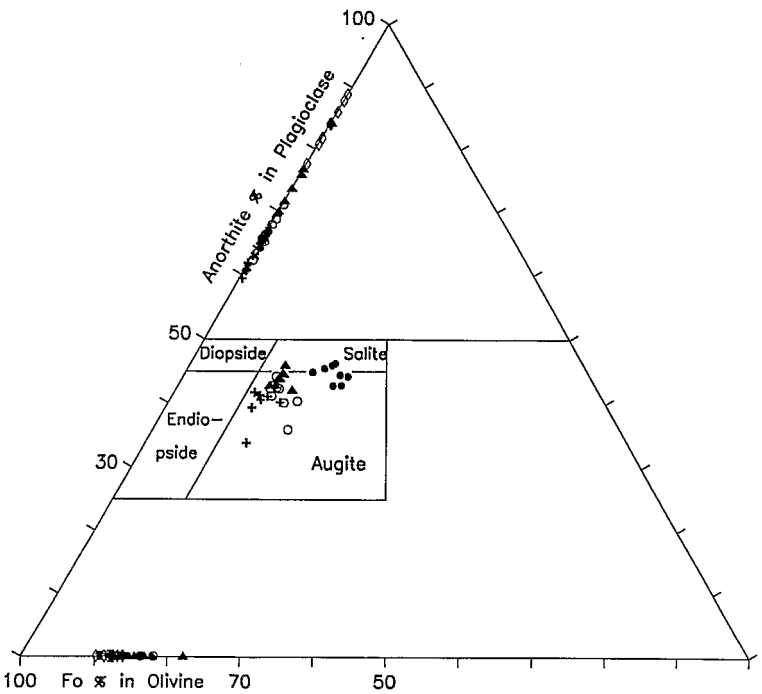

Fig. 9. Plagioclase, clinopyroxene and olivine compositions of the studied samples (microprobe analyses done by M. Bohn, on the CAMEBAX microprobe, "microsonde ouest" of Brest). Symbols used as follows: ◇ = sample 7-1; small arrow = sample 7-2; × = sample 7-4; + = sample 7-5; ● = sample 7-6; ○ = sample 7-7; ▲ = sample 7-8.

whose co-occurrence indicates an early Pleistocene biostratigraphic position (NN19a) with an estimated age of 1.87–1.35 Ma. *C. macintyrei* is absent in the other samples. The abundance of *E. huxleyi* in sample ST1-7-9c is indicative of the latest Pleistocene Zone NN21 (CN15) with an estimated age of less than 0.23 Ma. The position of the assemblages from samples ST1-7-9a, ST1-7-9b and ST1-7-10 is less precise. They are comprised between the extinction of *C. macintyrei* and the presence of *E. huxleyi*, that is within the interval NN19b–NN20. The NN19/NN20 boundary, usually defined by the extinction of *P. lacunosa*, cannot be placed here, because of the persistence of *P. lacunosa* till the end of the Pleistocene, as observed in the NN21 assemblage from the ST1-7-9c sample and also as previously noted in the South Fiji basin by Edwards (1973). Sample ST1-7-9a probably belongs to the lower part of Zone NN19b due to the abundance of *P. lacunosa* and the co-occurrence of *H. sellii*. Assemblages from samples ST1-7-9b and ST1-7-10 are characterized by the abundance of *Gephyrocapsa* with respect to *P. lacunosa* and the absence of *E. huxleyi*. This suggests a correlation to the upper part of Zone NN19b and to Zone NN20.

Analysis of sample ST1-7-9 in which three distinct assemblages were found, suggests a rather complex sedimentary history. First, the superposition of three assemblages correlated to Zones NN19b to NN21 (1.35 Ma to Present) indicates either a very low sedimentation rate or erosive processes occurring on the shallow plateau at the summit of the section. In addition, as indicated by the age of the assemblages found within the burrows, the growth of the manganese crust started most probably 0.3 Ma ago only.

4. Petrography and geochemistry of the basaltic rocks

Petrologic and mineralogic data relative to the lavas sampled during dive 7 are reported in Table 1. All the major types of lava observed during the dive have been sampled. They include 5 pillow lavas, 1 massive flow and 1 dike. All the samples but sample ST1-7-6 show slight alteration features, usually restricted to partial replacement of olivine by iddingsite with iron oxides and hydroxides. Additional informations from dive 8 which surveyed the middle part of the southern domain of the V-shaped graben (Fig. 4) are given for comparison. The three samples collected during this dive are very fresh, showing that this area was submitted to very recent volcanic activity.

Mineralogy

The mineralogy of these lavas is typical of basalts from oceanic spreading centers. The three deepest lava samples (ST1-7-1, 7-2, and 7-4) contain only phenocrysts of plagioclase and olivine with smaller opaque oxides (Cr-spinel and Ti-magnetite), whereas the other ones contain in addition clinopyroxene. Ilmenite was observed in one pillow core (ST1-7-6). The mineralogical compositions of the samples is summarized in Fig. 7. Olivines exhibit a relatively restricted range of Mg-rich compositions, ranging from Fo_{90} to Fo_{81}. Plagioclase compositions are more scattered. Phenocrysts from samples ST1-7-1 and 7-8 are Ca-rich (between An_{70} and An_{90}), whereas all the other compositions fall within the An_{60} to An_{70} range. Clinopyroxenes have dominantly augitic compositions, close to the diopside corner, except for sample ST1-7-6 where a slight iron enrichment towards salitic compositions can be noticed. These mineralogical variations have been plotted as a function of depth along the section (Fig. 10). Plagioclases from the intermediate levels generally show a lower calcium content than in the deepest and shallowest samples. Mg-content in the olivine tend to decrease regularly from the bottom to the summit of the section, whereas no general compositional trend appears for clinopyroxenes.

Geochemistry

Bulk rock ICP-AES analyses of major and trace elements are given in Table 2. When present, glass fragments from pillow rims have also been analysed with the microprobe for major elements (Table 2). Both glass and bulk rock compositions are in good agreement, showing that no important crystal accumulation or fractionation mechanisms occurred in these rocks.

Based on their mineralogy and major elements chemistry, most of these samples are similar to

TABLE 1

STARMER I dives 7 and 8: Summary of the sample morphology, mineralogy and modal content, lava types as distinguished in the text. G = glassy; GV = glassy to variolitic; FD = fine-grained dolerite; CD = coarse-grained dolerite. Mineralogy (PL = plagioclase; OL = olivine; CP = clinopyroxene; SP = Cr-rich spinel; MG = Ti-magnetite; CR = chromite; OP = MG + CR + ilmenite)

Sample number	Morphology	Depth	Texture	Mineralogy
ST I 7-1	Pillow	2881	GV	PL + OL + SP
ST I 7-2	Pillow	2868	GV	PL + OL + SP
ST I 7-3	Sediment	2726		
ST I 7-4	Pillow	2726	GV	PL + OL + MG + CR
ST I 7-5	Pillow center	2691	FD	PL + CP + MG
ST I 7-6	Pillow center	2590	FD	PL + CP + OL + OP
ST I 7-7	Massive flow	2366	FD	PL + CP + OL + MG
ST I 7-8	Dike	2222	GV	PL + CP + OL + MG
ST I 7-9	Sediment	2035		
ST I 7-10	Sediment	2033		
ST I 8-1	Pillow protuberance	2895	GV	PL + CP + OL
ST I 8-2	Pillow protuberance	2836	GV	PL + OL + SP
ST I 8-3	Sheet flow	2760	G	PL + OL + CP + SP

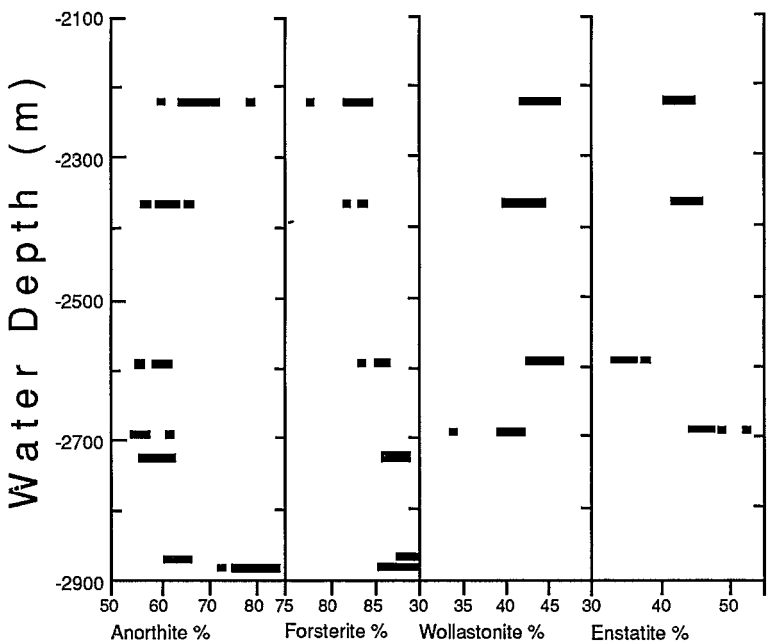

Fig. 10. Mineralogical and geochemical variations of the samples throughout the studied section.

N-type MORBs. They include some relatively more "primitive" compositions (e.g. samples ST1-7-1, and 7-2, with Mg number > 63), and a more "evolved" group (samples ST1-7-5, and 7-7; Mg number < 56). The two last samples have intermediate Mg numbers of about 60. However, samples ST1-7-4 and 7-6 also show relatively high Ni contents (358 and 278 ppm, respectively), although none of these analyses fits the characteristics of primary mantle derived magmas (Green et al., 1987). Most of these lavas are hyperstene and olivine normative, but only sample ST1-7-7 is

TABLE 2

Chemical analyses of the lava samples collected during the STARMER I dives 7 and 8 in the NFB triple junction area. Bulk rocks (BR) analyses (analyst: J. Cotten) obtained by A.A.S. for SiO_2, TiO_2, Al_2O_3, Fe_2O_3, MgO, CaO, Na_2O, K_2O, Ba, V, Cr, Co, Ni, Cu and Zn, by A.E.S. for MnO, Rb and Sr, colorimetry for P_2O_5, and ICP-AES for Sc, Y, Zr, Nb, La, Nd, Eu, Dy, Er and Yb (L.O.D. (3 σ) in ppm for these elements are: 0.5, 0.5, 1, 1, 1, 2, 0.2, 0.4, 1 and 0.2, respectively). Glass (G) analyses using the CAMEBAX microprobe of Brest (analyst: M. Bohn). For microprobe, the peak and background counting times was 6 s, and the filament current 15 kV

Cruise	STAR I	STAR I	STAR I	STAR I	STAR I	STAR I	STAR I	STAR I	STAR I	STAR I	STAR I	STAR I	STAR I
Sample	BR 7-1	G 7-1	BR 7-2	G 7-2	BR 7-4	G 7-4	BR 7-5	BR 7-6	BR 7-7	BR 7-8	BR 8-1	BR 8-2	BR 8-3
SiO_2	48.30	48.89	46.30	48.15	47.80	48.27	48.60	47.50	49.50	47.35	50.00	50.20	50.10
TiO_2	1.06	1.02	1.35	1.27	1.72	1.78	1.83	1.80	1.65	1.30	1.38	1.39	1.52
Al_2O_3	16.15	16.38	15.73	17.00	14.15	15.67	13.77	14.28	15.03	16.49	14.51	14.70	14.60
Fe_2O_3	9.19	8.88	8.80	9.39	10.12	9.75	12.49	10.55	9.75	9.26	10.45	10.45	10.55
MnO	0.15	0.16	0.14	0.15	0.13	0.19	0.17	0.15	0.16	0.14	0.18	0.18	0.18
MgO	9.02	9.02	10.04	11.50	10.40	8.96	5.99	9.18	6.85	7.60	7.59	7.69	7.43
CaO	12.73	12.42	12.48	10.53	9.56	10.02	11.33	9.97	12.11	12.62	12.21	11.82	11.96
Na_2O	2.26	2.44	2.70	2.77	2.93	2.98	2.89	2.86	2.78	2.74	2.82	2.73	2.96
K_2O	0.11	0.03	0.12	0.07	0.24	0.21	0.59	0.38	0.26	0.15	0.15	0.21	0.13
P_2O_5	0.05	0.12	0.08	0.07	0.15	0.21	0.10	0.10	0.10	0.05	0.08	0.10	0.10
Cr_2O_3		0.05		0.05		0.05							
H_2O^+	0.32		1.42		2.00		1.19	2.44	0.61	1.55	−0.52	−0.59	−0.50
H_2O^-	0.15		0.10		0.60		0.19	1.07	0.16	0.21	0.04	0.03	0.04
Total	99.49	99.39	99.26	100.96	99.80	98.08	99.14	100.28	98.96	99.46	98.89	98.91	99.07
Rb	3.5		3.5		4.0		18.0	5.0	7.5	6.0	4.0	5.5	3.5
Sr	86		220		215		146	260	168	323	122	148	141
Ba	26		26		18		24	14	40	12	25	42	40
V	229		189		227		240	228	273	219	257	264	263
Cr	336		336		302		137	260	270	260	207	207	209
Co	46		52		55		42	49	43	50	43	41	42
Ni	164		276		358		49	278	72	172	62	56	59
Sc	34.5		29.4		30.7		40.6	30.6	40.7	33.9	41.2	39.5	42.1
Y	24.4		25.3		31.9		38.5	33.0	33.3	26.2	31.5	29.9	33.2
Zr	44		88		119		103	127	91	67	74	81	88
Nb	1.0		1.2		3.5		3.3	3.5	5.0	1.0	2.7	5.2	3.2
La	1.4		3.3		6.2		5.0	6.4	5.7	2.2	3.7	5.2	4.6
Nd	6.2		9.0		13.6		11.8	14.2	11.3	8.0	9.7	9.9	10.4
Eu	0.71		0.98		1.19		1.15	1.22	1.12	0.93	0.95	0.93	1.09
Dy	3.9		4.3		5.2		6.1	5.4	5.3	4.2	5.2	4.8	5.4
Er	2.1		2.2		2.9		3.8	3.2	2.9	2.6	3.0	2.8	3.2
Yb	2.39		2.22		2.88		3.56	2.96	3.04	2.39	2.99	2.86	3.05

quartz normative and samples ST1-7-2 and 7-8 are nepheline normative, due mainly to their low silica content.

The composition of these samples is compared to N-MORBs as shown on Fig. 11, where selected large ion lithophile elements (LILE) and high field strength elements (HFSE) contents are plotted in a logarithmic diagram normalized to N-MORB (normalisation values after Sun and MacDonough, 1989). The compositions of rare earth and less incompatible elements of most of the samples (e.g. samples ST1-7-4, 7-5, 7-6, 8-1 and 8-3) are very close to those of N-MORBs which represent the dominant magma type described in the NFB (Eissen et al., 1991). However, a variety of geochemical signatures as early reported along the NFB spreading system (Eissen et al., 1994-this issue) is also found in this very restricted sample set. Based on the LILE contents, three groups can be distinguished. Samples ST1-7-7 and 8-2 are characterized by Ba, Rb, K, Sr, LREE enrichments relative to N-MORBs, but without Nb anomaly.

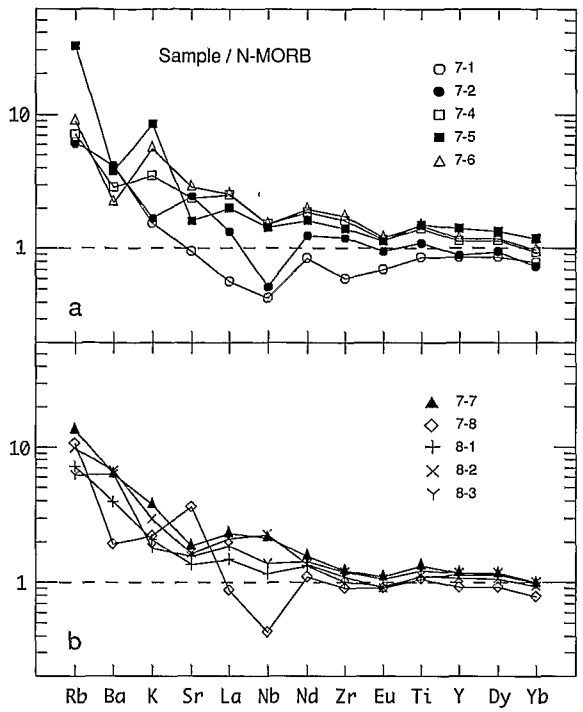

Fig. 11. Extended rare earth element abundances normalized to N-type MORBs (normalisation values from Sun and McDonough, 1989) for studied samples.

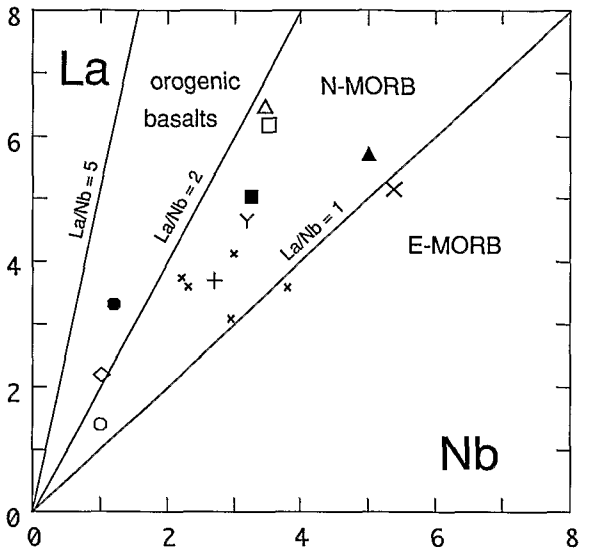

Fig. 12. Geodynamical environment of the studied basalts as indicated by the La versus Nb diagram. Fields are from Gill (1981). Same symbols as Fig. 9 except small crosses refering to other samples from the triple junction area (Eissen et al., 1994-this issue).

Their compositions are intermediate between N-MORBs and the transitional alkalic type described in the northern NFB (Price et al., 1990; Eissen et al., 1994-this issue), which tend toward E-MORB compositions. This trend is also found in two other samples coming from the triple junction area (Fig. 12) (samples MW5/4 of Price et al., 1990; and K17-1 of Eissen et al., 1994-this issue). High contents in Rb and K relatively to the other LILE, noticeable for samples ST1 7-5 and 7-6 (and to a lesser extend for samples ST1-7-4 and 7-8) are positively correlated with rather high LOI values (1.55–2.44%). This could result mainly from slight low temperature alteration. The third group includes samples ST1-7-1, 7-2 and 7-8, which show a remarkable negative Nb anomaly along with a clear LILE enrichment. On the La versus Nb diagram (Fig. 12), samples ST1-7-2 and 7-8 (and to a lesser extend 7-1) plot in the low-K orogenic field defined by Gill (1981), indicating affinity with magmas originated from subduction tectonic setting (Saunders and Tarney, 1984). These basalts also show geochemical signature close to the BABB-type as defined by Sinton and Fryer (1987).

5. Discussion and conclusions

Nature of the upper crust close to the 16°40'S triple junction

Dive no. 7 of the STARMER I cruise provided the opportunity to study an almost 800 m high continuous section through very young upper oceanic crust along the northern limit of the deep basin forming the eastern branch of the 16°40'S triple junction in the North Fiji Basin. The structural setting of the section is a topographic high (Figs. 2–4), with a complex morphology and an uncommon shallow depth (less than 2000 m). This abnormal setting suggests that this regional topographic high originated from outpourring of a very large volume of magma. The recent emplacement of the triple junction resulted in the break-apart of this topographic high (Tanahashi et al., 1991).

A number of volcanic facies have been encountered during the dive including massive and pillowed lavas and spectacular columnar-jointed

massive lavas. To our knowledge, these latter volcanic facies have been rarely observed in deep oceanic environment even in region such as the Pacific Rise where sheet-flows are abundant. Columnar-jointed sheet flows have been observed in the Western Mediterranean (Bellon et al., 1985) and along the western flank of the axial rift valley south of the eastern intersection of the Mid-Atlantic Ridge (MAR) with the Vema Fracture Zone (dive 7 of the *Nautile* cruise "Vemanaute"; Auzende et al., 1990). Columnar-jointed flows are also present on both flanks of the axial valley north of the western intersection between the MAR and the 15°20'N Fracture Zone (*Nautile* cruise "Faranaute"; M. Cannat and H. Bougault, pers. commun., 1993). Basaltic and andesitic colonnades are known in the extrusive series of the northeastern Troodos ophiolite of Cyprus (Schmincke and Bednarz, 1990a). Such flows are interpreted to have been emplaced during the magmatic stage of the magmatic/tectonic cycle responsible for the construction of the ophiolite at the spreading center. This stage is characterized by a high eruptive rate and is followed by periods of extension and fracturing of the massive flows and emplacement of pillow lavas at lower eruptive rates.

In the observed section, the ratio between massive, sheet flows and pillow basalts is high, as pillows have been observed only at the base and at the top of the section. This confirms that the crust in this area grew mostly during a stage of high eruptive rate, as early suggested by the abnormal elevation of the oceanic crust in the surveyed area.

The occurrence of a sheeted dike complex at 2254 m (Fig. 5) gives rise to the question of the continuity of the observed section. Two interpretations can be presented. We may first consider that the dikes represent the upper part of the classical dike complex of typical oceanic crustal sections as found in most complete ophiolites (Oman, Cyprus, ...). In such a case, the pillowed and massive lavas which were observed below during the dive must have been down faulted along sub-vertical normal fault planes. The occurrence of numerous cataclastic breccias associated with faults and schistozed basalts observed during the first part of the dive confirms that the crust exposed below the dikes, from 2600 to 2350 m, suffered significant deformation. Considering that the terrace observed at 2038 m represents the top of the oceanic crust in the area, this hypothesis would imply that the total thickness of the pillow lavas is only 100 m. This value seems very low, according to the fact that the surveyed area is located within a volcanic domain characterized by high topography and thus by a relatively thick crust.

We thus favour a second interpretation, in which the dikes do not represent the top of a classical "dike complex" but an isolated set of sheeted dikes, probably the feeders of overlying flows. Such feeder dikes have been observed in the central parts of sheet-flow volcanoes of the Troodos ophiolite (Schmincke and Bednarz, 1990).

These observations allow us to further discuss some aspects of the deformation of this very young oceanic crust. The abundance of vertical tectonic breccias observed during the first part of the dive confirms that the basal part of the wall can be regarded as a major tectonic boundary along which significant vertical and strike-slip motions occurred (Fig. 13). Along the upper part of the section, we also observed numerous fault scarps devoid of thick cataclastic breccias. All along the dive, low angle faults were never observed. This indicates that very little horizontal displacement occurred between the floor of the graben and the volcanic plateau to the north of the wall. Assuming that the floor of the basin situated at the foot of the wall (2900 m) was originally at the same elevation as the top of the volcanic plateau north of the wall (1900 m), a minimum vertical offset of 1000 m occurred along a deformed area with a maximum width of 700 m (Fig. 13). Most of the deformation is probably concentrated within a 200 m wide zone, that is along the faults associated with cataclastic breccias observed from 2600 to 2300 m. Finally, we emphasize that the deformation linked to the brutal subsidence of the graben occurred along a narrow vertical simple shear zone without affecting the surrounding crust.

Age of the crust, geodynamical implications

The results of the micropaleontological study of the samples collected during dive no. 7 show that

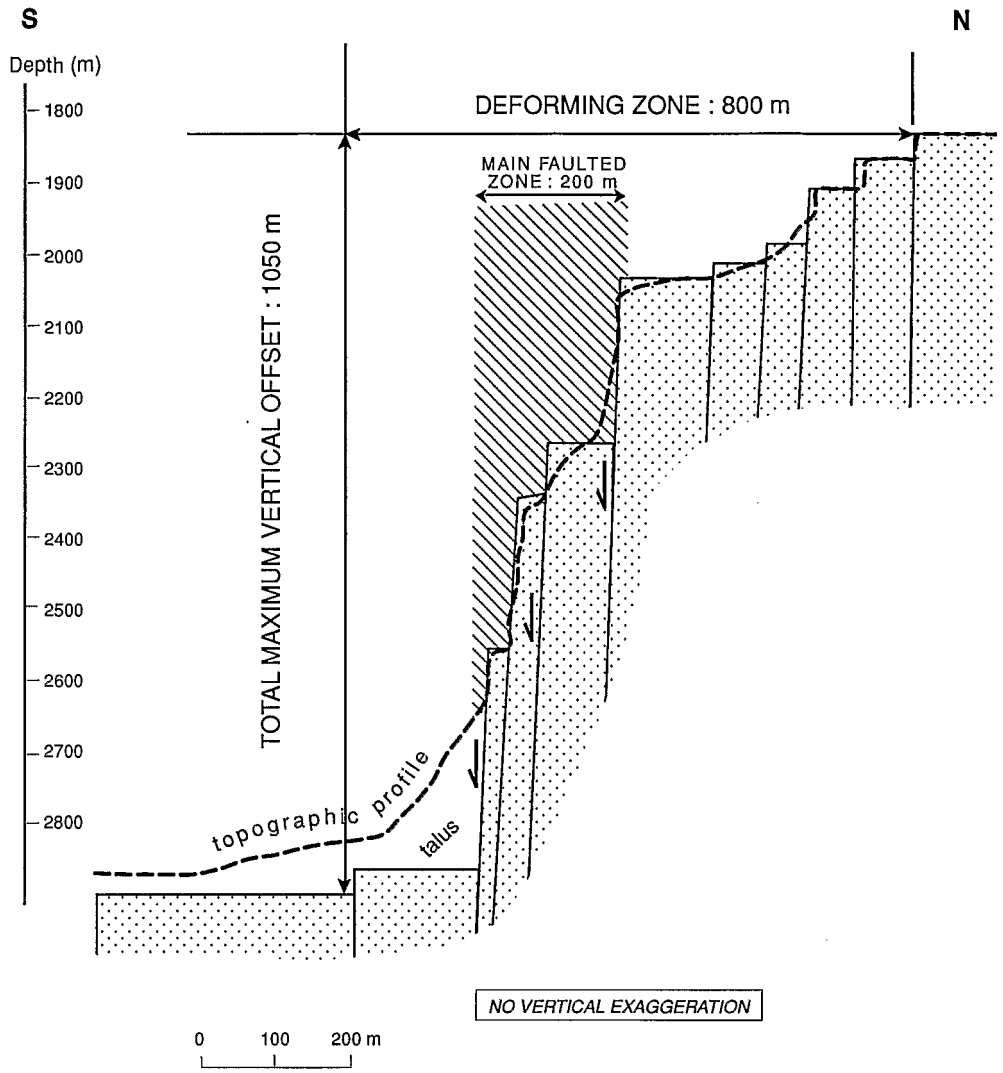

Fig. 13. Synthetic cross-section of the cliff with location of the main deformation zone.

the oceanic crust in the surveyed area is at least as old as 1.9–1.3 Ma, based on the age of sample ST1-7-3. Unfortunately this sample was not collected in situ. The age of the sedimentary cover of the pillow basalts observed at the summit of the northern wall of the graben is at least 1.3 Ma as indicated by the age of the different assemblages found in samples ST1-7-9(a,b,c) and ST1-7-10.

The studied section is located 20 km to the west of the present-day N160° spreading axis, the active northern branch of the triple junction (Auzende et al., 1991b). If we assume that the observed crust was emplaced along this axis at least 1.9 Ma ago as suggested by the oldest assemblage found in the sedimentary samples, the half rate of spreading along this segment can be estimated to 1.1 cm/yr. This value is not in good agreement with values deduced from the analysis of the magnetic anomalies. Half rates of 2.5 and 2.3 cm/yr have been calculated for the northern and southern spreading axis in the vicinity of the triple junction, respectively, based on the width of the axial magnetic anomaly (0–0.7 Ma) (Auzende et al., 1990a; Gràcia-Mont, 1991). According to these values, the crust in the surveyed area should be around 0.5 Ma old. Estimation based on magnetic anoma-

lies 2A to 1 at 18°10'S along the southern active axis indicate an average half spreading rate of 2.6 cm/yr over the last 3.4 Ma (Auzende et al., 1990b).

A possible explanation to the relatively old age of the crust in the surveyed area is that this portion of the North Fiji Basin was created along an old spreading axis, now inactive, located farther west. Such hypothesis has been proposed previously by Lafoy et al. (1990), on the basis of morphological and kinematic considerations. According to these authors, a N–S trending spreading axis was active before 1 Ma to the west of the present-day triple junction. At 1 Ma, sinistral strike slip motion started along the North Fiji Fracture Zone, i.e. along the eastern branch of the triple junction, in response to oceanic accretion in the northern part of the Lau basin (Auzende et al., 1988b). This caused the jump of the northern and southern segments of the ridge toward the east, the opening of extensional grabens at the triple junction, and the propagation of a volcanic ridge into the triple junction graben.

Geochemistry of the lavas

Basalts from the NFB are dominently N-MORBs. But basalts with E-MORBs compositions, intermediate between transitional alkalic types and N-MORBs, have been recovered from the northern part of the basin (Price et al., 1990). Likewise, several basalts sampled between 15°S and 18°30'S, along the N15° and N160° segments of the central active spreading axis of the NFB, show BABBs affinities, with a more or less pronounced Nb negative anomaly. At last, between 18°30'S and 21°S, the N–S segment of the central active spreading axis of the NFB produces only N-MORBs (Eissen et al., 1994-this issue).

Lavas collected during STARMER dive 7 along this upper-crustal section, as well as during dive 8 in the middle part of the V-shaped graben include N-MORB, E-MORB and BABB types. They thus show similar chemical diversity of magmas as described for the entire NFB. N-MORBs is the "normal" magma type produced at the axis of a mature spreading center, and is frequently found in back arc basins locally associated with other magma types (Hawkins and Melchior, 1985; Saunders and Tarney, 1984; Sinton and Fryer, 1987; Boespflug, 1990). It has been suggested that the E-MORBs of the NFB result from the mixing of an alkali-rich source (Rotuma type) and an N-MORB depleted source (Price et al., 1990; Eissen et al., 1994-this issue). It is noticeable that the alkali-rich character decreases from 13°N towards 18°30'S where it complitely vanishes. BABBs with LILE-enrichment and Nb negative anomaly are also typically produced in back-arc settings. They possibly result of the interaction between lithospheric mantle and fluids and/or melts derived from a subducting slab beneath the basin (Saunders and Tarney, 1984; Sinton and Fryer, 1987). However, in the central region of the NFB, far away from any active margin, the presence of BABBs cannot be directly attributed to the presence of an active subduction zone.

We thus propose that the melts produced in the central NFB originated from an heterogeneous mantle, possibly at the scale of few kilometers, and basically consisting of three components: (1) a depleted lithospheric component, (2) a enriched lithospheric component, part of which had previously interacted with fluids and/or melts from a subducted slab, and (3) an alkali-enriched component. Most of the geodynamical models explaining the evolution of the New-Hebrides/Fiji/Lau system refer to the presence of an old continuous subduction zone, now inactive, corresponding to the Vitiaz lineament to the north of the NFB. The southward subduction of the Pacific plate under the Vitiaz trench stopped at least at 12 Ma when the Ontong–Java Plateau collided with the Vitiaz arc (Falvey, 1978; Auzende et al., 1988c). This collision probably led to a subsequent reversal of the subduction polarity and to the rotation of some parts of the Vitiaz arc now forming the Fiji Islands basement and the roots of the New-Hebrides arc. We propose that this subduction led to the metasomatic enrichment in incompatible elements of the overlying mantle wedge. Part of this metasomatized mantle was later involved in the melting processes leading to the generation of the central NFB basalts in general, and more specifically in the 16°40'S triple junction area. As suggested by Eissen et al. (1994-this issue), the

alkali-enriched source could connect to the deep source involved in the magma genesis of the volcanic alkali lineaments found north of the NFB.

Acknowledgements

This work was supported by grants from UBO/IFREMER contracts 1990–1991. We thank captain M. Delmas, the crew of the R/V *Nadir* and the *Nautile* team for their help during the STARMER I cruise. We also thank R.C. Maury for helpful comments on a first version of the manuscript and A. Nicolas and R.C. Maury for constructive reviews. J.L. Travers helped in preparing the photographs. We also thank M. Bohn for assistance in performing microprobe analyses.

References

Auzende, J.M., Eissen, J.P., Gente, P., Lafoy, Y., Lagabrielle, Y., Schaaf, A. and Charlou, J.L., 1988a. The accretion system of the central part of the North Fiji Basin (SW Pacific) between 16°40'S and 21°S (SEAPSO Leg 3 cruise—Dec. 1985). Tectonophysics, 146: 317–351.

Auzende, J.M., Eiichi, H., Boespflüg, X., Deo, S., Eissen, J.P., Hashimoto, J., Huchon, P., Ishibashi, J., Iwabushi, Y., Jarvis, P., Joshima, M., Kisimoto, K., Kiuwahara, Y., Lafoy, Y., Matsumoto, T., Mazé, J.P., Mitsuzawa, K., Momma, H., Naganuma, T., Nojiri, Y., Ohta, S., Otsuka, K., Okuda, Y., Ondréas, H., Otsuki, A., Ruellan, E., Sibuet, M., Tanahashi, M., Tanaka, T. and Urabe, T., 1988b. L'accrétion récente dans le Bassin Nord-Fidjien: premiers résultats de la campagne franco-japonaise Kaiyo 87. C. R. Acad. Sci. Paris, Sér. II, 306(1): 971–978.

Auzende, J.M., Lafoy, Y. and Marsset, B., 1988c. Recent geodynamic evolution of the North Fiji Basin (SW Pacific). Geology, 16: 925–929.

Auzende, J.M., Urabe, T., Deplus, C., Eissen, J.P., Grimaud, D., Huchon, P., Ishibashi, J., Joshima, M., Lagabrielle, Y., Mével, C., Naka, J., Ruellan, E., Tanaka, T. and Tanahashi, M., 1989. Le cadre géologique d'un site hydrothermal actif: La campagne STARMER I du submersible Nautile dans le bassin Nord-Fidjien. C. R. Acad. Sci. Paris, Sér. II, 309: 1787–1795.

Auzende, J.M., Bideau, D., Bonatti, E., Cannat, M., Honnorez, J., Lagabrielle, Y., Malavieille, J., Mamaloukas-Frangoulis, V. and Mével, C., 1990a. The MAR-Vema Fracture Zone intersection surveyed by deep submersible *Nautile*. Terra Nova, 2: 68–73.

Auzende, J.M., Eiichi, H., Boespflüg, X., Deo, S., Eissen, J.P., Hashimoto, J., Huchon, P., Ishibashi, J., Iwabushi, Y., Jarvis, P., Joshima, M., Kisimoto, K., Kiuwahara, Y., Lafoy, Y., Matsumoto, T., Mazé, J.P., Mitsuzawa, K., Monma, H., Naganuma, T., Nojiri, Y., Ohta, S., Otsuka, K., Okuda, Y., Ondréas, H., Otsuki, A., Ruellan, E., Sibuet, M., Tanahashi, M., Tanaka, T. and Urabe, T., 1990b. Active spreading and hydrothermalism in North Fiji Basin (SW Pacific). First results of Japanese French cruise. Mar. Geophys. Res., 12: 269–282.

Auzende, J.M., Urabe, T., Bendel, V., Deplus, C., Eissen, J.P., Grimaud, D., Huchon, P., Ishibashi, J., Joshima, M., Lagabrielle, Y., Mével, C., Naka, J., Ruellan, E., Sibuet, M., Tanaka, T. and Tanahashi, M., 1991a. In situ geological and geochemical study of an active hydrothermal site on the North Fiji Basin ridge. In: K.A.W. Crook (Editor), The Geology, Geophysics and Mineral Resources of the South Pacific. Mar. Geol., 98: 259–269.

Auzende, J.M., Okuda, Y., Bendel, V., Ciabrini, J.P., Eissen, J.P., Gràcia-Mont, E., Hirose, K., Iwabuchi, Y., Joshima, M., Kisimoto, K., Lafoy, Y., Lagabrielle, Y., Marumo, K., Matsumoto, T., Mitsuzawa, K., Momma, H., Mukai, H., Naka, J., Nojiri, Y., Ortega-Osorio, A., Ruellan, E., Tanahashi, M., Tupua, E. and Yamagushi, K., 1991b. Propagation en échelon de la dorsale du Bassin Nord-fidjien entre 16°40 et 14°50'S (Yokosuka–Starmer). C. R. Acad. Sci. Paris, Sér. II, 312: 1531–1538.

Bellon, H., Maury, R., Bellaiche, G., Réhault, J.P., Mermet, J.F. and Auzende, J.M., 1985. Age et nature des formations volcaniques prismées observées et préle vées dans le Canyon des Moines (Sud-Ouest Corse) pendant la campagne Cyaligure. Mar. Geol., 67: 163–176.

Bendel, V., Fouquet, Y., Urabe, T., Auzende, J.M., Lagabrielle, Y., 1991. Hydrothermal deposits in the North Fiji Basin: petrology and geochemistry (STARMER). STARMER Symp. (Nouméa, New Caledonia, February 7–11, 1991.) Abstr.

Boespflüg, X., 1990. Evolution géodynamique et géochimique des bassins arrière-arc. Exemple des bassins d'Okinawa, de Lau et Nord-Fidjien. Thèse Doct., Univ. de Bretagne Occidentale, Brest.

Edwards, A.R., 1973. Calcareous nannofossils from the Southwest Pacific, Deep Sea Drilling Project, Leg 21. Init. Rep. DSDP, 21: 641–691.

Eissen, J.P., Lefèvre, C., Maillet, P., Morvan, G. and Nohara, M., 1991. Petrology and geochemistry of the central North Fiji Basin spreading center (SW Pacific) between 16°40'S and 22°S. In: K.A.W. Crook (Editor), The Geology, Geophysics and Mineral Resources of the South Pacific. Mar. Geol., 98: 201–239.

Eissen, J.P., Nohara, M., Cotten J. and Hirose K., 1994. The North Fiji Basin basalts and their magma sources: part 1. Trace and rare earth elements constraints. In: J.-M. Auzende and T. Urabe (Editors), North Fiji Basin: STARMER French–Japanese Program. Mar. Geol., 116: 153–178.

Falvey, D.A., 1978. Analysis of paleomagnetic data from the New Hebrides. Aust. Soc. Explor. Geophys. Bull., 9: 117–123.

Francheteau, J., Armijo, R., Cheminée, J.L., Hékinian, R., Lonsdale, P. and Blum, N., 1992. Dyke complex of the East Pacific Rise exposed in the walls of Hess Deep and the structure of the upper oceanic crust. Earth Planet. Sci. Lett., 111: 109–121.

Gill, J.B., 1981. Orogenic Andesites and Plate Tectonics. Springer, Berlin, York, 390 pp.

Gràcia-Mont, E., 1991. Etude morphostructurale du segment N160 de la dorsale du bassin nord-fidjien. Analyse des données de la campagne Yokosuka 90. DEA Rep., Univ. Bretagne Occidentale, Brest, France. (Unpubl.)

Green, D.H., Falloon, J.J. and Taylor, W.R., 1987. Mantle-derived magmas—role of variable source peridotite and variable C–H–O fluid compositions. In: B.O. Mysen (Editor), Magmatic Processes: Physio-chemical Principles. Univ. Park, PA, Geochem. Soc. Spec. Publ., 1, pp. 139–154.

Grimaud, D. and Ishibashi, J.I., 1991. Chemical features of the hot waters emitted at the White Lady active vents. STARMER Symp. (Nouméa, New Caledonia, February 7–11, 1991.) Abstr.

Hawkins, J.W. and Melchior, J.T., 1985. Petrology of Mariana Trough and Lau Basin basalts. J. Geophys. Res., 90: 11431–11468.

Hills, S.J. and Thierstein, H.R., 1989. Plio-Pleistocene calcareous plankton biochronology. Mar. Micropaleontol., 14: 67–96.

Juteau, T., Bideau, D., Dauteuil, O., Manach, G., Naidoo, D., Nehlig, P., Ondreas, H., Tivey, M.A. and Whipple, K., 1991. The western Blanco transform: preliminary insights into the oceanic crustal architecture and transform zones processes. EOS, 72(44): 519 (abstr.).

Karson, J.A. and Dick, H.J.B., 1983. Tectonics of ridge–transform intersections at the Kane fracture zone. Mar. Geophys. Res., 6: 51–98.

Kroenke, L.W. and Shipboard Scientific Party, 1987. Cruise Report. CCOP/SOPAC North Fiji Basin expedition. R/V Moana Wave Cruise MW 87-01, 37 pp.

Lafoy, Y., 1989. Evolution géodynamique des bassins marginaux Nord-Fidjien et de Lau (Sud-Ouest Pacifique). Thèse, Univ. Bretagne Occidentale, Brest, France, 261 pp.

Lafoy, Y., Auzende, J.M., Ruellan, E., Huchon, P., Honza, E., 1990. The 16°40'S triple junction in the North Fiji Basin (SW Pacific). Mar. Geophys. Res., 12: 285–296.

Lagabrielle, Y., Mamaloukas-Frangoulis, V., Cannat, M., Auzende, J.M., Honnorez, J., Mével, C. and Bonatti, E., 1992. Vema Fracture Zone (Central Atlantic): tectonic and magmatic evolution of the Median Ridge and the eastern ridge transform intersection. J. Geophys. Res., 97(B12): 17331–17351.

Mamaloukas-Frangoulis, V., Auzende, J.-M., Bideau, D., Bonatti, E., Cannat, M., Honnorez, J., Lagabrielle, Y., Malavieille, J., Mével, C. and Needham, H.D., 1991. In situ study of the Eastern Ridge–Transform Intersection of the Vema Fracture Zone. Tectonophysics, 190: 55–72.

Martini, E. and Müller, C., 1986. Current Tertiary and Quaternary calcareous nannoplankton stratigraphy and correlations. Newsl. Stratigr., 16: 99–112.

Mével, C., Cannat M., Gente P., Marion E., Auzende J.-M. and Karson, J.A., 1991. Emplacement of deep rocks on the west Median Valley Wall of the MARK area. Tectonophysics, 190: 31–53.

Okada, H. and Bukry, D., 1980. Supplementary modification and introduction of code numbers to the low-latitude coccolith biostratigraphic zonation (Bukry, 1973; 1975). Mar. Micropaleontol., 5: 321–325.

OTTER, Oceanographer Tectonic Research Team, Karson, J.A., Fox, P.J., Sloan, H., Crane, K.T., Kidd, W.S.F., Bonatti, E., Stroup, J.B., Fornari, D.J., Elthon, D., Hamlyn, P., Casey, J.F., Gallo, D.G., Needham, D. and Sartori, R., 1984. The geology of the Oceanographer Transform: The ridge–transform intersection. Mar. Geophys. Res., 6: 109–141.

Perch-Nielsen, K., 1985. Cenozoic calcareous nannofossils. In H.B. Bolli, J.B. Saunders and K. Perch-Nielsen (Editors), Plankton Stratigraphy. Cambridge Univ. Press, pp. 427–554.

Price, R.C., Johnson, L.E. and Crawford, A.J., 1990. Basalts of the North Fiji Basin: the generation of back arc basin magmas by mixing of depleted and enriched mantles sources. Contrib. Mineral. Petrol., 105: 106–121.

Ruellan, E., Auzende, J.M., Honza, E. et al., 1989. L'accrétion dans le bassin Nord Fidjien méridional: premiers résultats de la campagne franco-japonaise STARMER/KAIYO 88. C. R. Acad. Sci. Paris, Sér. II, 309: 1247–1254.

Saunders, A.D. and Tarney, J., 1984. Geochemical characteristics of basaltic volcanism within back-arc basins. In: B.P. Kokelaar and M.F. Holwells (Editors), Marginal Basins Geology, Volcanic and Associated Sedimentary and Tectonic Processes in Modern and Ancient Marginal Basins. Blackwell, Oxford, pp. 59–76.

Schminke, H.U. and Bednarz, U., 1990. Pillow, sheet flow and breccia flow volcanoes and volcano-tectonic hydrothermal cycles in the extrusive series of the northeastern Troodos ophiolite (Cyprus). In: J. Malpas, E.M. Moores, A. Panayiotou and C. Xenophontos (Editors), Ophiolites, Oceanic Crustal Analogues. Proc. Symp. (Troodos, 1987.) pp. 185–206.

Sinton, J.M. and Fryer, P., 1987. Mariana trough lavas from 18°N: Implications for the origin of back arc basin basalts. J. Geophys. Res., 92, 12: 782–802.

Sun, S.S. and McDonough, W.F., 1989. Chemical isotopic systematics of oceanic basalts. In: A.D. Saunders and M.J. Norry (Editors), Magmatism in the Ocean Basins. Geol. Soc. Spec. Publ., 42: 313–345.

Tanahashi, M., Kisimoto, K., Joshima, M., Lafoy, Y., Honza, E. and Auzende, J.M., 1991. Geological structure of the central spreading system, North Fiji basin. In: K.A.W. Crook (Editor), The Geology, Geophysics and Mineral Resources of the South Pacific. Mar. Geol., 98: 187–200.

Reprinted from

MARINE GEOLOGY

INTERNATIONAL JOURNAL OF MARINE GEOLOGY, GEOCHEMISTRY AND GEOPHYSICS

Marine Geology, 116 (1994) 113–132
Elsevier Science B.V., Amsterdam

Geology and geochemistry of a 800 m section through young upper oceanic crust in the North Fiji Basin (Southwest Pacific)

Yves Lagabrielle[a], Jean-Marie Auzende[b,1], Jean-Philippe Eissen[c], Marie-Christine Janin[d] and Joseph Cotten[a]

[a]*URA CNRS 1278 and GDR "GEDO", Faculté des Sciences, Université de Bretagne Occidentale, 6, Avenue Le Gorgeu, 29287 Brest Cédex, France*
[b]*IFREMER, Centre de Brest and GDR "GEDO", B.P. 70, 29280 Plouzané, France*
[c]*ORSTOM, Centre de Brest and GDR "GEDO", B.P. 70, 29280 Plouzané, France*
[d]*CNRS and Université P. and M. Curie, Laboratoire de Micropaléontologie, 4, Place Jussieu, T15, E4, 75252 Paris Cédex 05, France*

(Received October 2, 1992; revision accepted June 14, 1993)

ELSEVIER